



Contents lists available at ScienceDirect

# Spectrochimica Acta Part A: Molecular and Biomolecular Spectroscopy

journal homepage: [www.elsevier.com/locate/saa](http://www.elsevier.com/locate/saa)

## Growth and characterization of an organic single crystal: 2-[2-(4-Diethylamino-phenyl)-vinyl]-1-methyl-pyridinium iodide



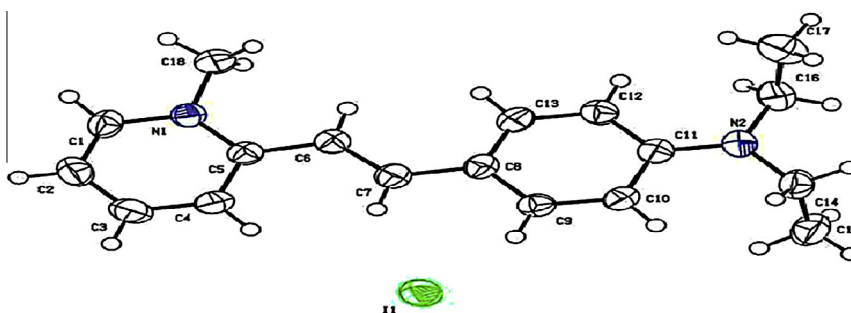
K. Senthil, S. Kalainathan\*, A. Ruban Kumar

Centre for Crystal Growth, School of Advanced Sciences, VIT University, Vellore 632 014, Tamil Nadu, India

### HIGHLIGHTS

- Highly good transparent single crystals with size up to  $10 \times 7 \times 3 \text{ mm}^3$  have been harvested by slow evaporation technique.
- $^1\text{H}$  and  $^{13}\text{C}$  NMR confirms the molecular structure of the DEASI crystal.
- Crystal has good transparency in visible–NIR region.
- From the TGA curve of this sample shows that material is highly stable up to 262 °C.
- Refractive index, mechanical, dielectric, etching studies were carried out.

### GRAPHICAL ABSTRACT



### ARTICLE INFO

#### Article history:

Received 20 November 2013  
 Received in revised form 13 January 2014  
 Accepted 22 January 2014  
 Available online 5 February 2014

#### Keywords:

Chemical synthesis  
 Optical materials  
 FT-IR  
 Crystal growth  
 Mechanical studies

### ABSTRACT

Optically transparent crystal of the organic salt DEASI (2-[2-(4-Diethylamino-phenyl)-vinyl]-1-methyl-pyridinium iodide) has been synthesized by using Knoevenagel condensation reaction method. The synthesized material has been purified by successfully recrystallization process. Single crystals of DEASI have been grown by slow evaporation technique at room temperature. The solubility of the title material has been determined at different temperature in acetonitrile/methanol mixture. The cell parameters and crystallinity of the title crystal were determined by single crystal XRD. The powder diffraction was carried out to study the reflection plane of the grown crystal and diffraction peaks were indexed. The presence of different functional groups in the crystal was confirmed by Fourier transform infrared (FTIR) analysis.  $^1\text{H}$  NMR spectrum was recorded to confirm the presence of hydrogen nuclei in the synthesized material. The optical property of the title crystal was studied by UV–Vis–NIR spectroscopic analysis. The melting point and thermal property of DEASI were studied using TGA/DSC technique. The Vicker's hardness ( $H_v$ ) was carried out to know the category. The dielectric constant and dielectric loss of the compound decreases with an increase in frequencies. Chemical etching studies showed that the DEASI grows in the two dimensional growth mechanisms. The Kurtz–Perry powder second harmonic generation (SHG) test has done for title crystal.

© 2014 Elsevier B.V. All rights reserved.

### Introduction

The wide range of organic nonlinear optical crystals has been investigated due to their potential applications in signal processing, optoelectronics, laser technology, bioimaging, optical data

\* Corresponding author. Tel.: +91 416 2202350; fax: +91 416 2243092.  
 E-mail address: [kalainathan@yahoo.com](mailto:kalainathan@yahoo.com) (S. Kalainathan).

storage for the development of technologies in telecommunication and data processing [1–4]. Organic materials exhibit large nonlinear response when compared to inorganic materials because of the presence of  $\pi$ -conjugated system linked by appropriate electron releasing groups (ERGs) and electron withdrawing groups (EWGs) at their two ends, which can enhance the asymmetric electronic charge distributions in the system. The asymmetric charge distributions between such groups leading to capable of generating second harmonic frequency, and which is playing the key step in the field of photonics [5–7]. In recent years, the efforts have been investigated towards the synthesis of novel  $\pi$  conjugated organic molecules because of their second and third-order nonlinear optical activities, large optical damage threshold, low frequency dispersion and fast response time [8–10]. Organic stilbazolium crystals have a relatively high probability because of their highly aligned and stable orientation of NLO chromospheres in the crystal system [11]. For the past few years, the ionic organic material is a particular interest, because of their thermal stability and photochemical stability, and its mechanical properties in the field of photonics [12,13]. The development of organic highly polar ionic stilbazolium crystals is based on the presence of strong coulomb interactions [13]. Recently stilbazolium family crystals are of considerable attention due to their attractive large nonlinear optical properties, a large electrooptic coefficient and low dielectric constant. One of the main advantages of organic materials is that the structure can be altered by suitable substituted electron donor and electron acceptor groups in their  $\pi$ -conjugated system compared to inorganic materials [8,14]. There are different methods for crystal growth. It is known that the slow evaporation solution

growth technique is commonly used for the growth of organic and inorganic crystals.

In the present investigation, we report the synthesis, growth of a stilbazolium derivative, 2-[2-(4-Diethylamino-phenyl)-vinyl]-1-methyl-pyridinium iodide single crystals. These crystals were successfully grown by the slow evaporation technique. The grown title crystal has been subjected to different characterizations such as single crystal X-ray diffraction studies, powder XRD, FTIR,  $^1\text{H}$  NMR,  $^{13}\text{C}$  NMR, UV-Vis NIR, refractive index, thermal, dielectric studies, chemical etching and Vicker's microhardness measurements.

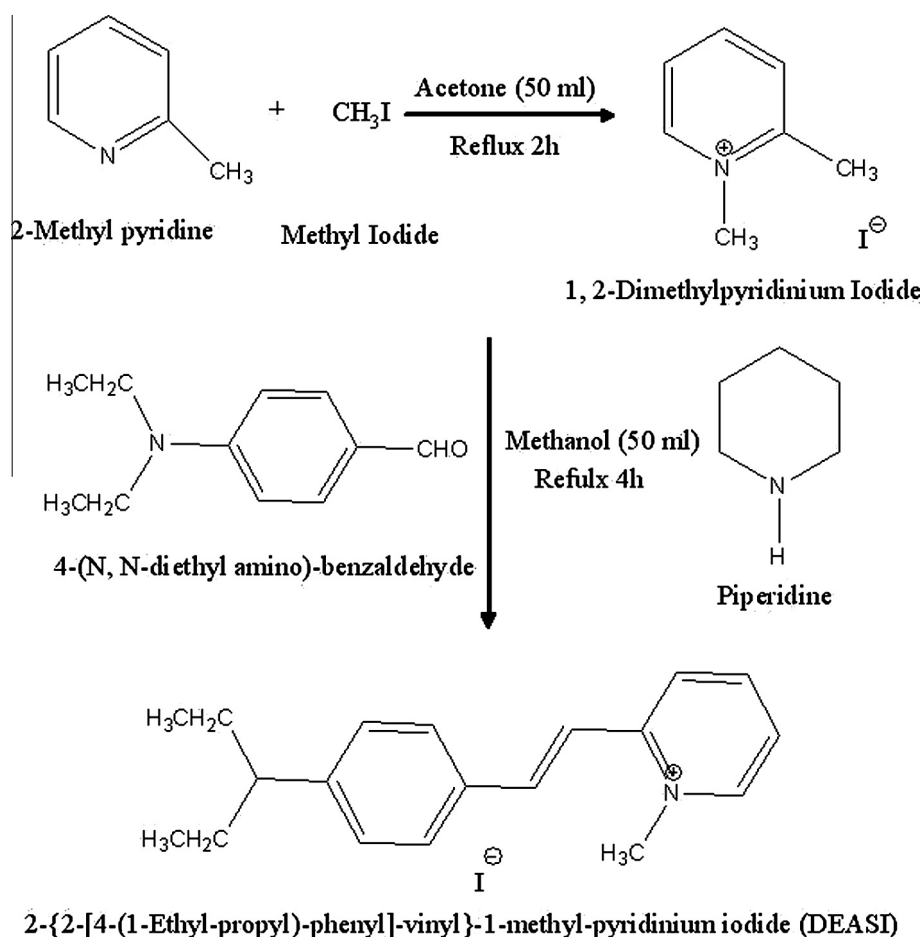
## Experimental procedure

### Material synthesis

The title material was synthesized by Knoevenagel condensation of 1,2-Dimethylpyridinium iodide, which was prepared from 2-methylpyridine and methyl iodide and 4-(N, N-diethyl amino)-benzaldehyde in the presence of piperidine. The overall synthesis process and molecular structures are given in Scheme 1.

#### 1,2-Dimethylpyridinium iodide (A)

The equimolar ratio of 2-methylpyridine (8 ml, 80 mmol) and methyl iodide (5.2 ml, 80 mmol) was added in dried acetone (50 ml). The whole mixture was taken in a two-neck flask (250 ml) fitted with thermometer and condenser. Then the mixture was refluxed at 60 °C for 2 h until it pale white precipitate crystallized. The resulting salts were collected by filtration, and the salt was washed with diethyl ether to removing of unreacted starting



Scheme 1. Synthesis process of DEASI.

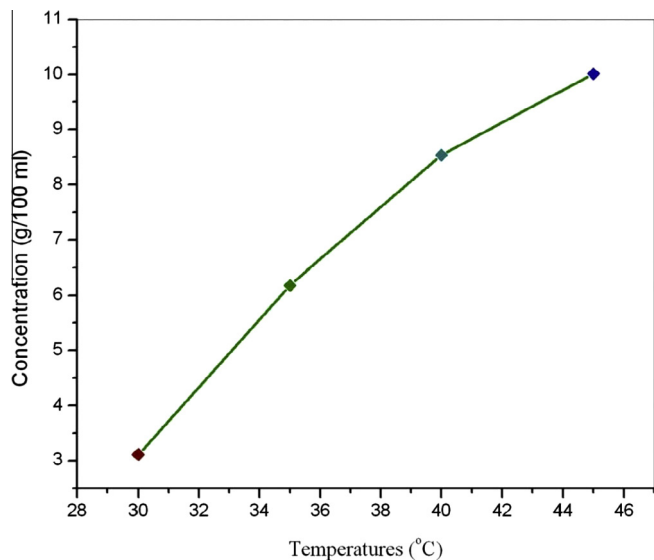


Fig. 1. Solubility curve of DEASI crystal in methanol–acetonitrile solvent system.

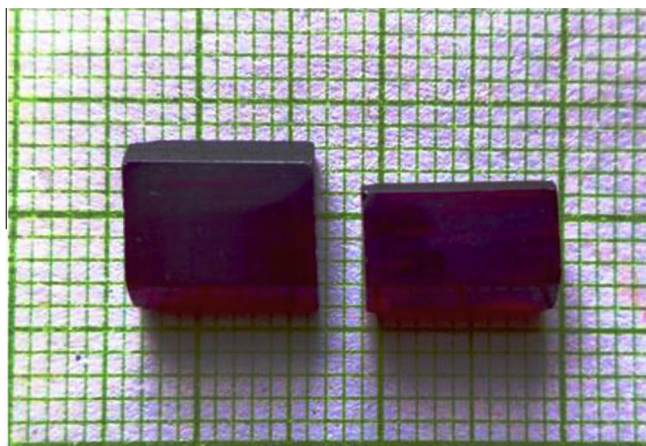


Fig. 2. As grown crystal of DEASI.

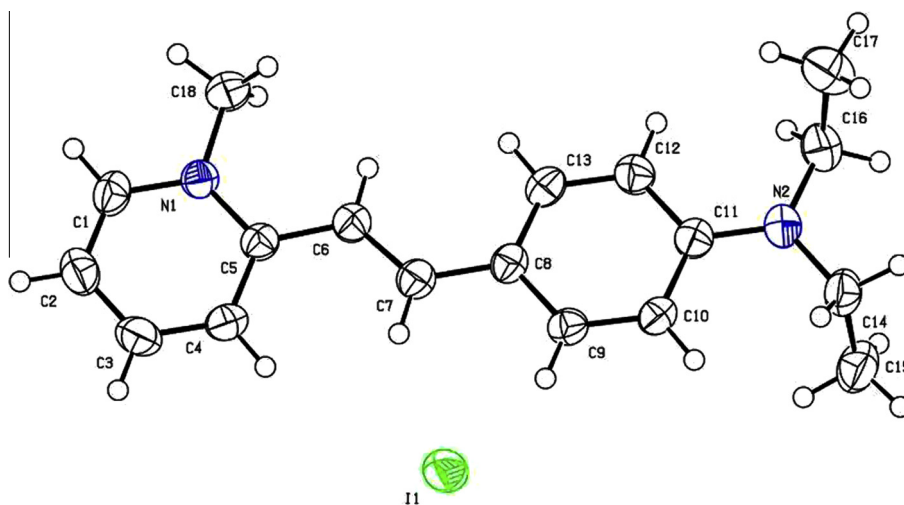


Fig. 3. Ortep diagram of – [2-(4-Diethylamino-phenyl)-vinyl]-1-methyl-pyridinium iodide.

materials. The pale white salt dried at the oven, and it had a melting point at 155 °C.

#### 2-[(E)-4-(Diethyl amino) styryl]-1-methyl-pyridinium iodide (B)

The title material (B) was prepared by previously reported method [15]. The equimolar ratio of **A** (7.052 g, 30 mmol) and 4-(N, N-diethyl amino)-benzaldehyde (5.317 g, 30 mmol) in a dried methanol (50 ml) was placed in round bottom flask. After the addition of the above mixture, the piperidine was added as a catalyst and the mixture solution refluxed for 4 h under nitrogen atmosphere. The resulting red precipitate suspension was cooled and then precipitate was filtered off and finally washed with diethyl ether to remove the starting material. The final product was then successively recrystallized using mixture solvent methanol–acetonitrile (1:1).

#### Solubility

Thermodynamically, the chemical potential of the purified salt is equal to the chemical potential of the same solute in the saturated solution. The determination of solubility measurement is one of the decisive factors for crystal growth technique since it decides estimation of solubility amount of material and temperature. The solubility of DEASI was investigated in different solvents such as methanol, ethanol, acetone, methanol–acetonitrile, methanol–acetone, and acetonitrile–ethanol mixed solvent. Interestingly the solubility of DEASI is very high in methanol–acetonitrile mixed solvent system, and hence that solvent system was used as a growth process. The solubility of DEASI salt was determined for different temperatures from 30 to 45 °C by dissolving the solute in 100 ml of methanol–acetonitrile (1:1) solvent mixture in an air tight container maintained at a constant temperature with continuous stirring to get the saturated solution. A solution of 10 ml was taken in a Petri dish and dried up till to get rid of solvents. By measuring the dried salt in the dish, the solubility at a relevant temperature was calculated by using the formula [16].

$$\text{Solubility (Wt\%)} = \frac{\text{wt(solute)}}{\text{Wt(solute + solvent)}} \times 100.$$

The solubility of the title compound at different temperatures as exposed in Fig. 1. From the graph, it is seen that the solubility linearly increases with the increase of temperature.

**Table 1**  
Single crystal XRD data of DEASI.

Empirical formula	C <sub>18</sub> H <sub>23</sub> I N <sub>2</sub>
Formula weight	394.28
Crystal system	Monoclinic
Space group	P2(1)/c
a (Å)	7.8282(2) Å
b (Å)	20.3830(4) Å
c (Å)	11.0259(2) Å
α	90°
β	92.4780(10)°
γ	90°
Volume (Å <sup>3</sup> )	1757.67(6)
Molecules per unit cell (Z)	4
Calculated density (Mg/m <sup>3</sup> )	1.490
Absorption coefficient (mm <sup>-1</sup> )	1.818

**Crystal growth**

Crystal growth was performed by slow evaporation solution growth technique. Based on the solubility data, a saturated solution of DEASI was dissolved in methanol–acetonitrile mixed solvent system (3.08 g in 50 ml) at 35 °C. The solution was filtered using fine pore Whatman filter paper. The filtered solution was kept in a 100 ml beaker, and it was tightly covered with aluminum foil with few holes for slow evaporation rate of the solvent, and it was kept at 35 °C in a constant temperature water bath. After a period of 10 days of solvent evaporation, good transparent single crystals with dimension up to 10 × 7 × 3 mm<sup>3</sup> have been harvested. The as grown single crystals are shown in Fig. 2.

**Characterization studies**

Single crystal X-ray diffraction study was examined to confirm the crystal system and the lattice parameter values of the DEASI single crystal using Bruker Kappa APEX II diffractometer with Mo Kα radiation (λ = 0.71073 Å). The powder XRD pattern was carried out on a BRUKER X-ray diffractometer with the Cu Kα radiation (λ = 1.5406 Å) in the range of 10–80°, at the scanning rate of 0.02° S<sup>-1</sup> (2θ). The functional groups vibration of DEASI crystals were recorded in the range of 4000–400 cm<sup>-1</sup> using SHIMADZU IRAFFINITY spectrometer by the pressed KBr pellet technique. The formation of molecular structure of DEASI crystal has been confirmed by using BRUKER instrument operating with 400 MHz model FT-NMR spectrometer, and DMSO-d<sub>6</sub> was used as a solvent. The optical transparency of DEASI single crystal was checked using ELICO SL 218 double beam UV–Vis–NIR spectrometer in the range of 190–1100 nm. The TGA/DSC study was carried out for the title crystal using Netzsch Sta-449F3 analyzer, and in the temperature range of 35 °C to 500 °C at a heating rate of 10 °C/min in a nitrogen atmosphere. The mechanical strength of grown crystal was determined using MH-112 Viker’s microhardness diamond indenter at ambient temperature. The dielectric response of the grown crystal was analyzed using HIOKI 3532 50 LCR HTESTER instrument for different temperatures at various frequencies. Etching studies were analyzed on the (010) plane of the DEASI crystal using Carl Zeiss optical microscope.

**Result and discussions**

*Single crystal X-ray diffraction analysis*

Single crystal X-ray diffraction analysis was carried out to determine the crystal structure and to determine lattice parameter values. The structure was solved and refined by full matrix least square technique using the SHELX97 program. It is observed that

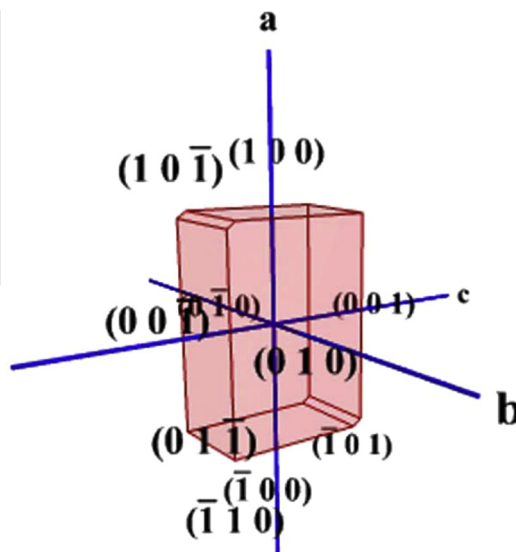


**Fig. 4.** Morphology of DEASI.

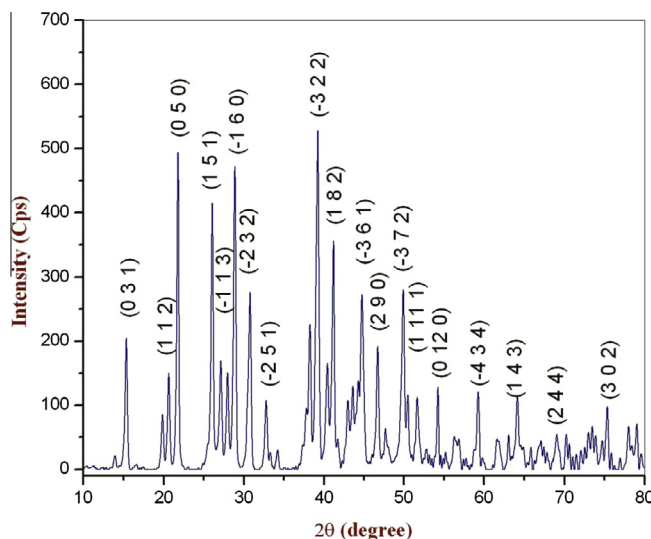


**Fig. 5.** Indexed powder XRD pattern of DEASI.

**Table 2**  
Powder XRD data for DEASI.

Pos [2Th.]	d-Spacing d (Å)	Height [cts]	Area	FWHM	hkl
15.385	5.7545	333.5	4898.9	0.2953	031
20.631	4.30169	238.8	3770.7	0.3134	112
21.789	4.07566	811.4	10138.1	0.2557	050
26.076	3.41453	672.3	8911.7	0.2695	151
27.15	3.28175	265.6	4739.4	0.3585	-113
28.905	3.08646	745.3	11664.3	0.3218	-160
30.801	2.9006	429.1	8339.9	0.3856	-232
32.809	2.72756	166.5	3019.6	0.3538	-251
39.267	2.29254	805.7	17000.6	0.4186	-322
41.225	2.18807	542.9	8879.2	0.331	182
44.785	2.02206	404.9	9716.3	0.4819	-361
46.752	1.94145	283.2	5030.1	0.355	290
49.947	1.82449	412.2	8960.1	0.4333	-372
51.692	1.76693	159.1	3863.7	0.4735	1111
54.272	1.68886	186.7	2496.8	0.266	0120
59.315	1.55674	170.7	3305.2	0.385	-434
64.209	1.4494	157.1	3745.9	0.4771	143
69.055	1.35903	74.6	2516.6	0.6524	244
75.376	1.25997	134	2402.4	0.3682	302

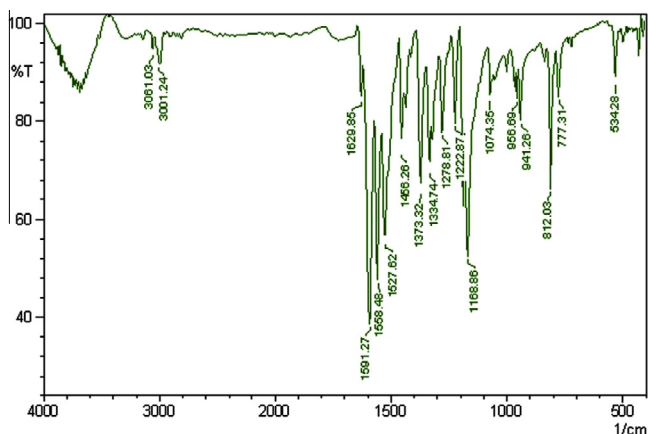


Fig. 6. FTIR spectrum of DEASI.

the compound crystallizes in the monoclinic crystal system with space group  $P2(1)/c$ , and the obtained lattice parameters values,  $a = 7.8282 (2) \text{ \AA}$ ,  $b = 20.3830 (4) \text{ \AA}$ ,  $c = 11.0259 (2) \text{ \AA}$ ,  $V = 1757.67 (6) \text{ \AA}^3$  and  $Z = 4$ . The obtained single crystal XRD data of the present work confirmed the structure of the grown DEASI crystal (Fig. 3-Ortep diagram). Thus, the obtained results are in good agreement with the literature [15]. The single crystal data of DEASI is presented in Table 1. Morphology of the grown crystal was indexed using WinXMorph program [16,17]. The indexed morphology of DEASI crystal is shown in Fig. 4.

#### Powder X-ray diffraction

To confirm the crystalline nature of the grown crystals, powder X-ray diffraction analysis of the sample were carried out. The observed powder XRD pattern has been indexed by POWDER X software program. The indexed powder X-ray diffraction pattern for DEASI is given in Fig. 5. The observed sharp and well defined Bragg's peaks at specific  $2\theta$  angle shows the good crystallinity of DEASI crystal. The Table 2 shows the powder X-ray diffraction data of title material.

#### FTIR spectral analysis

The recorded FTIR spectrum of the DEASI is shown in Fig. 6. The peaks at  $3001.24$  and  $3061.01 \text{ cm}^{-1}$  are attributed to the aromatic C–H stretching vibrations. The obtained stretching band at  $1629.85 \text{ cm}^{-1}$  due to the C=C stretch vibration in the DEASI compound. The observed band between  $1527.62$  and  $1591.27 \text{ cm}^{-1}$  is attributed to the stretching vibrations in the aromatic rings. The peak at  $1456.26 \text{ cm}^{-1}$  is corresponds to the  $\text{CH}_2$  bending mode. The band found at  $1373.32$ , and  $1334.74 \text{ cm}^{-1}$  are assigned to the  $\text{CH}_3$  bending absorption and C–N stretching mode. The peak at  $956.69 \text{ cm}^{-1}$  is corresponds to the 1, 2 substituted pyridinium ring. The observed peaks that are between  $500\text{--}700 \text{ cm}^{-1}$  are expected to the out-plane of ring bending modes, and in-plane ring deformation modes are observed between  $1100$  and  $1200 \text{ cm}^{-1}$  [18,19]. Thus, the FTIR studies confirm the presence of the key functional group of DEASI.

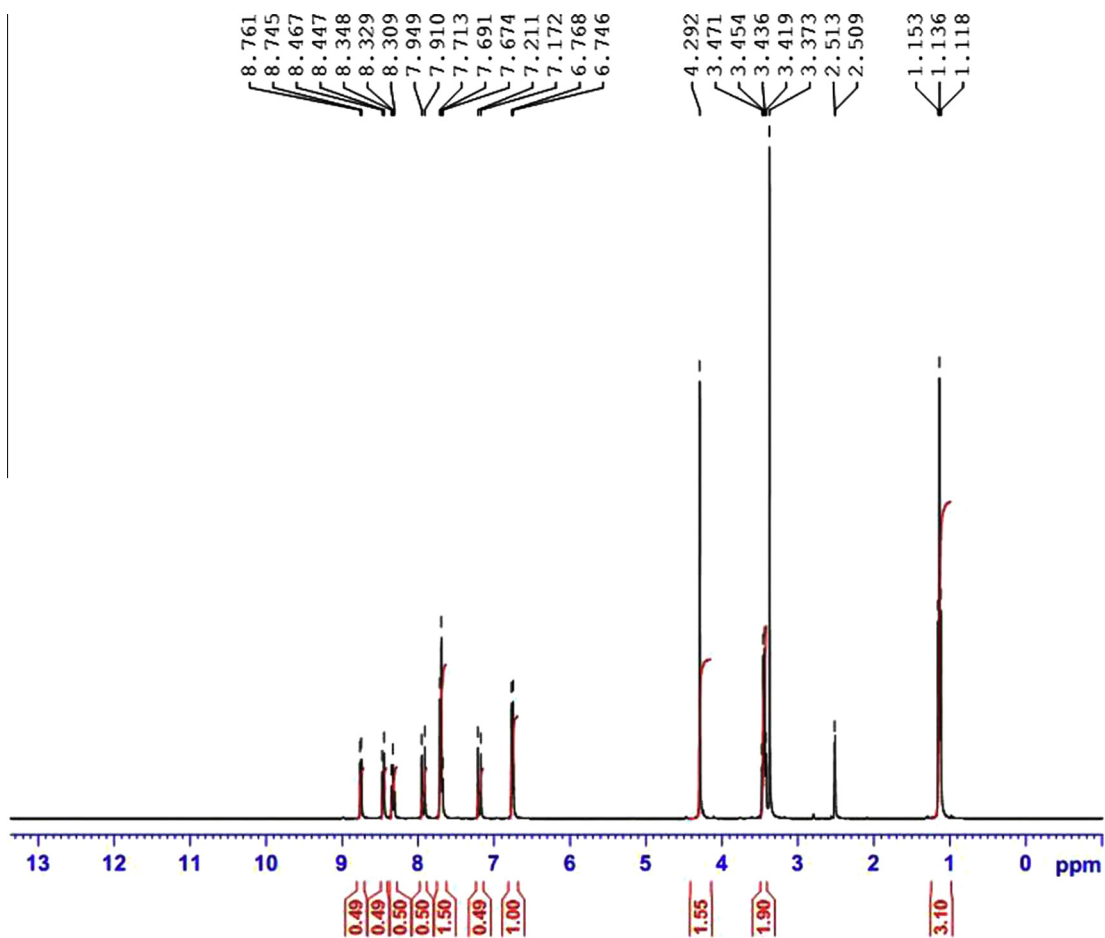


Fig. 7.  $^1\text{H}$  NMR spectrum of DEASI.

**<sup>1</sup>H and <sup>13</sup>C NMR spectral analysis**

<sup>1</sup>H NMR and <sup>13</sup>C NMR spectral studies have been carried out to confirm the formation of the synthesized materials and their molecular structure of the grown crystal. From the <sup>1</sup>H NMR spectrum of DEASI, the triplet at 1.136 is due to the six N-(CH<sub>2</sub>CH<sub>3</sub>)<sub>2</sub> hydrogens. The quartet peak at 3.436 is due to the four hydrogens of the N-(CH<sub>2</sub>CH<sub>3</sub>)<sub>2</sub>. The singlet peak at 4.292 is ascribing to the three hydrogens of N-CH<sub>3</sub>. The chemical shift (δ) at 3.373 is due to the water molecule. The quintet observed at 2.50 is due to the solvent ((CD<sub>3</sub>)<sub>2</sub>S=O). The two doublet signals at 7.212 and 7.910 are due to the two olefinic hydrogens (HC=CH). The two doublet peak lie at 6.746 and 7.691 are ascribed to the four hydrogens of the N-(CH<sub>2</sub>CH<sub>3</sub>)<sub>2</sub>=C<sub>6</sub>H<sub>4</sub> aromatic ring. The two doublet peaks of a pyridinium ring produced at 8.447 and 8.745. The triplet observed around 8.329 is due to the sixth position hydrogen of the pyridinium ion of DEASI. So, the formation the title compound was confirmed by proton NMR spectral analysis and it is shown in Fig. 7.

The recorded <sup>13</sup>C NMR spectrum of DEASI is shown in Fig. 8. The peak at 12.45 ppm and 43.85 ppm are attributed to the methyl group, and 45.62 ppm is assigned to the methylene group in the title material. The pyridinium ring carbon is observed from the peaks at 131.12 ppm, 142.90 ppm and 149.70 ppm. There are peaks nine found at, 109.86, 112.22, 121.56, 122.56, 123.41, 142.90, 144.18, 145.16, 153.26 ppm, which are corresponds to the formation of vinyl carbon and aromatic ring.

**UV-Vis NIR optical absorption spectral analysis**

The optical absorption spectrum for the grown DEASI crystals was recorded in the crystal (thickness 2 mm was used) as well as

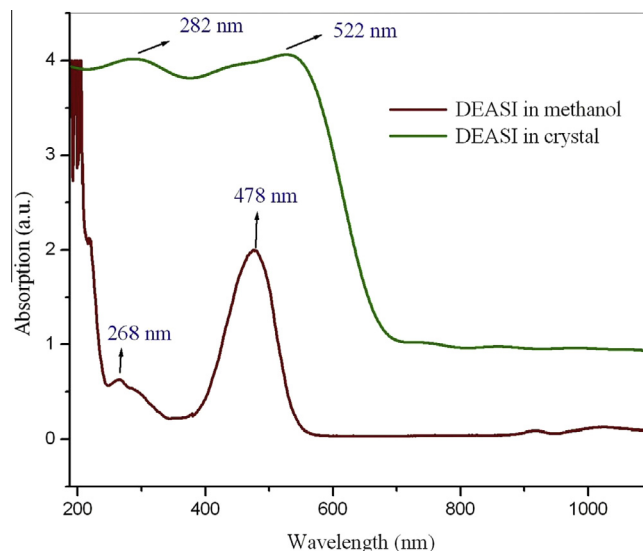


Fig. 9. UV-Vis NIR spectrum of DEASI.

in methanol solution, and the obtained spectrum is as shown in Fig. 9. The absorption spectrum of the DEASI crystal and its solution phase are shown in the same figure for the comparison. The absorption spectrum of DEASI crystal in methanol shows two different absorption peaks and the appearance of this kind of peaks were reported by Kumar et al. and Jagannathan and Kalainathan [20,21]. The minor absorption peak at 268 nm corresponds to the

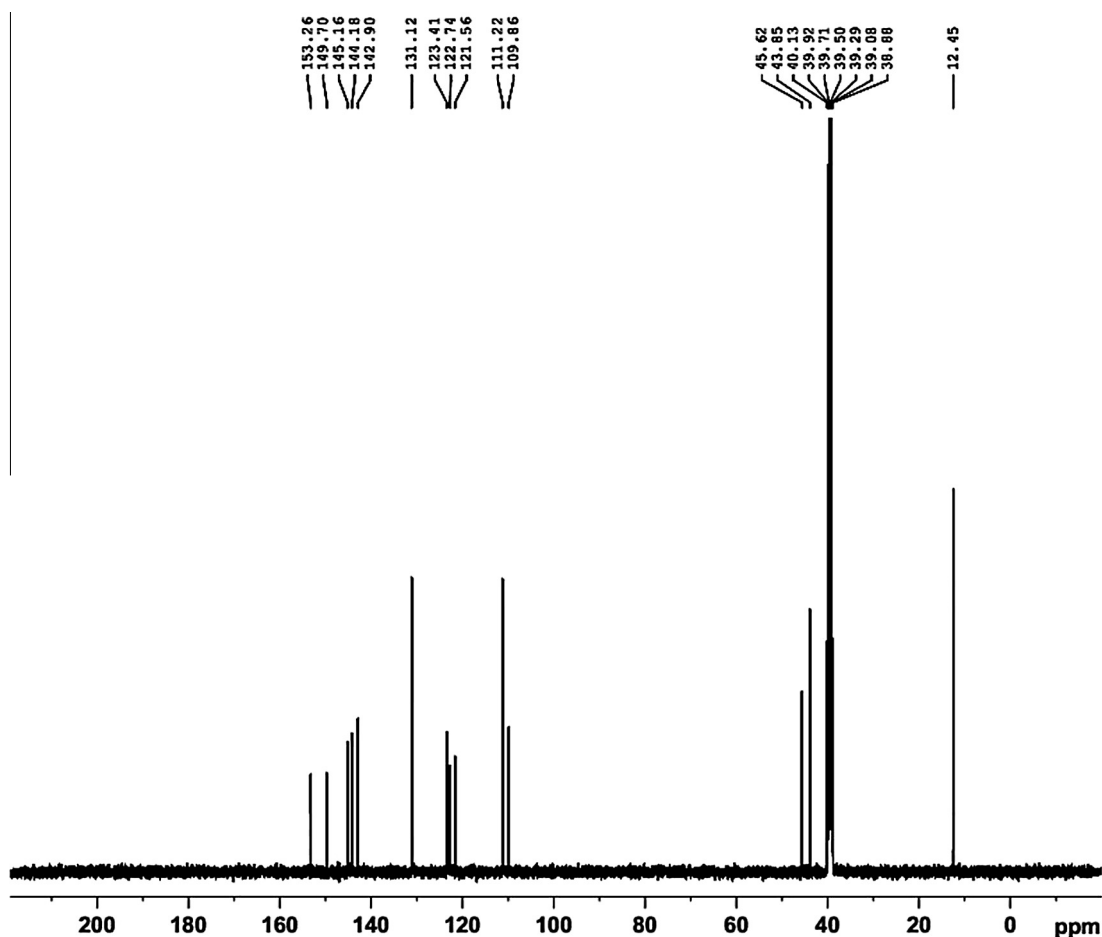


Fig. 8. <sup>13</sup>C NMR spectrum of DEASI.

$n-\pi^*$  transition which is indicating to the pyridinium group present in the crystal system, and main absorption peak at 478 nm corresponds to the  $\pi-\pi^*$  transitions of the extended conjugated system (stilbazolium chromophore) which causes the material absorbs light in the Vis–NIR range.

#### Refractive index

The refractive index measurement of the crystal is one of the useful parameters for optical studies. The refractive index of the title crystal was measured using Abbe refractometer (ATAGO, NAR-4T, Japan) connected by digital thermometer with thermistor cable connector jack, and the instrument was designed use at the wavelength of the sodium D line (589.3 nm). The Abbe refractometer was pre-calibrated by measuring the refractive indices of toluene and benzene. Crack free and optically clear surface of the grown crystal was chosen for the study. Few drops of methylene iodide were allowed on both the prism surface and crystal surface which make close contact between crystal and prism. The crystal was placed between two prisms (measuring and illuminating). Light passes through the crystal from the illuminating prism (sodium lamp) gets reflects on the bottom surface of reflector prism. The telescope was used to evaluate the location of the margin between dark and light region. The refractive index of DEASI crystal was measured at room temperature, and the measured refractive index was found to be 1.647.

#### Thermo gravimetric analysis (TGA) and differential scanning calorimetry (DSC) studies

The thermo gravimetric analysis (TGA) and differential scanning calorimetric analysis (DSC) are very useful characterization technique to study the phase transition, different stages of decompositions and thermal stability of the materials. The powdered crystal sample 1.769 was used for the initial analysis. The final residual mass of the experiment was 5.31% of the initial mass at 498.1 °C. The resulting TGA and DSC spectrum of DEASI is shown in Fig. 10. From the figure, the DSC curve shows a sharp endothermic peak at 276.6 °C. The sharpness of the endothermic peak confirms the melting point of the specimen and good crystalline perfection of the synthesized compound. The TGA curve of this sample shows

that material is highly stable up to 262 °C, and there is no phase transition up to 262 °C, and it is also indicating that the absence of the water molecule in the material. The major weight loss of about 57.37% in the temperature range 262–268 °C due to the complete decomposition of the stilbazolium ion. After that, the remaining 35.56% molecules decomposed and volatilization above 312 °C. A very broad peak observed at 310.8 °C attributed to the change in the physical state of the crystal. Thus, the TGA and DTA analysis confirm the stability of the material, and which makes a potential material for laser applications and fabrication of any optical devices below its melting point.

#### Mechanical properties

Good optical quality of the crystals and mechanical properties are playing a main role in device applications. Mechanical strength of the crystal depends on the various parameters such as lattice energy, Debye temperature, interatomic spacing composition of the crystalline solids. The transparent well polished smooth surface of the grown crystal was selected, and it was subjected to static indentation tests made at ambient temperature and loads varied from 10 to 100 g were used for making indentations with indentation time of 5 s in all cases. The Vicker's micro hardness ( $H_v$ ) profile of crystal is calculated from the standard equation.

$$H_v = 1.8544(P/d^2) \text{ kg/mm}^2, \quad (1)$$

Here,  $H_v$  is the Vickers hardness number in kg/mm,  $P$  is the applied load in kg and  $d$  is the mean diagonal length in mm of the indentation impression. The variation of hardness number ( $H_v$ ) with the applied load ( $P$ ) is shown in Fig. 11. It is evident from the curve that increase in microhardness gradually with an increase in applied loads up to 100 g, and further increase crack develop on the smooth surface of the grown crystal due to the release of internal stresses generated locally by indentation [22]. The Meyer's index number was calculated from the Meyer's law, which relates the applied load ( $P$ ) and indentation diagonal length ( $d$ ) as  $P = k_1 d^n$

$$\log P = \log k + n \log d \quad (2)$$

where  $k$  is the material constant and  $n$  is the Meyer's index. In order to find the value of 'n', the graph is plotted against  $\log P$  vs.  $\log d$  (Fig. 12), which provides a straight line. The slope of this straight

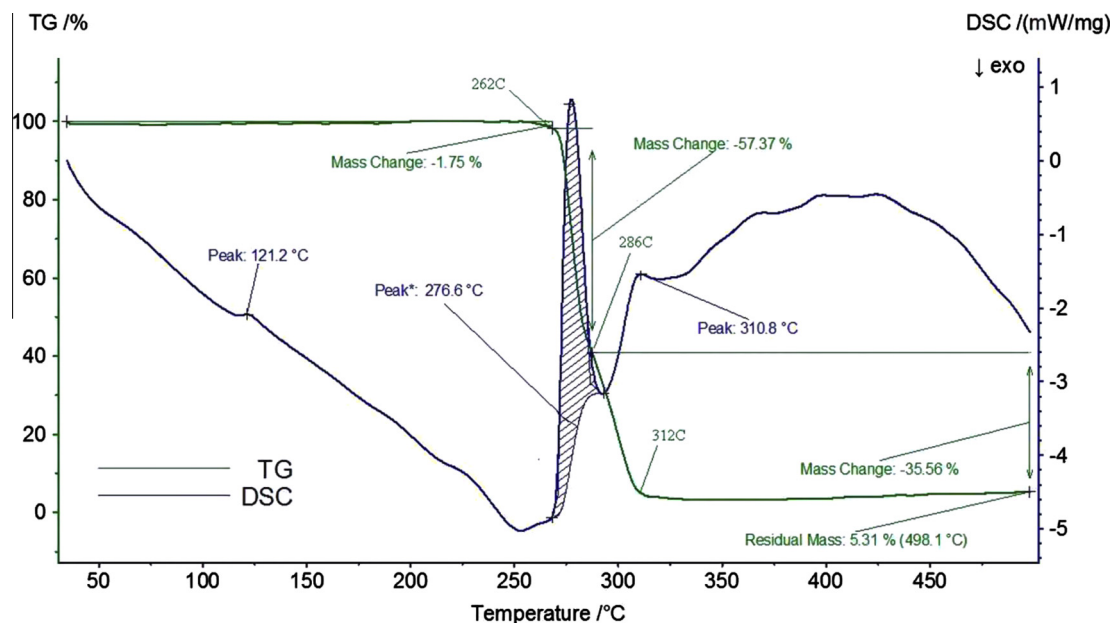


Fig. 10. TGA/DSC curve of DEASI.

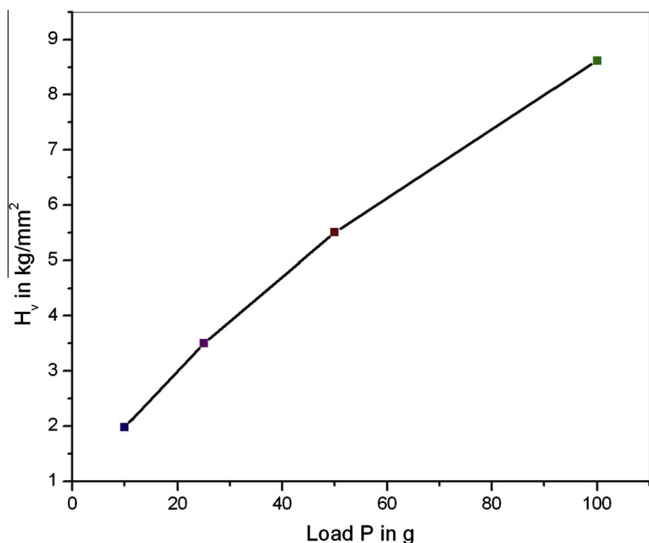


Fig. 11. Variation of hardness number ( $H_v$ ) with load ( $P$ ) for DEASI crystal.

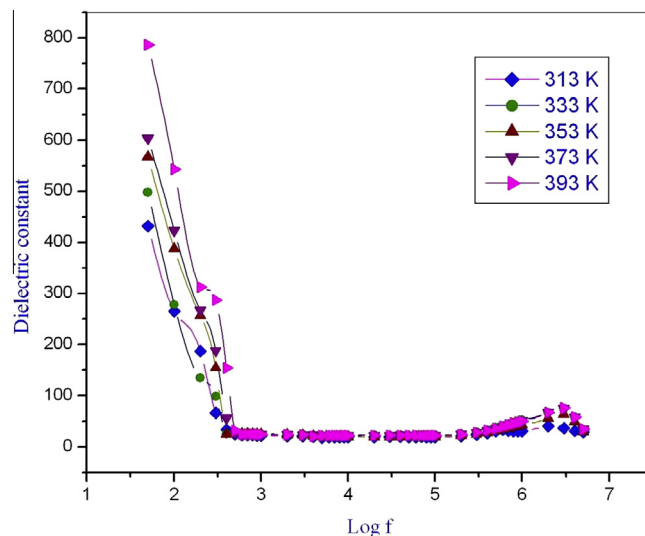


Fig. 13. Variation of dielectric constant with log frequency at different temperatures for DEASI single crystal.

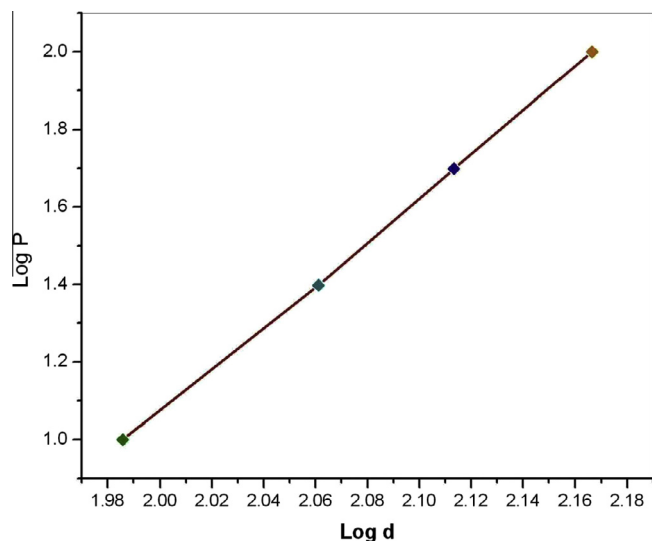


Fig. 12. Graph between  $\text{Log } P$  and  $\text{Log } d$ .

line gives the Mayer's index number ' $n$ '. The calculated value of  $n$  is 5.28.  $H_v$  should increase with the increase of  $P$  if  $n > 2$  and decrease if  $n < 2$ . According to the concept of Onitsch ' $n$ ' should lie between 1 and 1.6 for harder material and above 1.6 for softer materials [23,24]. Thus, DEASI crystal belongs to the soft material category.

#### Dielectric studies

Dielectric properties are correlated with the lattice dynamics in the crystal and electro-optic property of the crystals particularly when they are non conducting materials [25]. Hence, the prominent (010) faces of defect free and transparent DEASI single crystals of 3 mm thickness were subjected to dielectric studies at different temperatures for various frequencies ranging from 50 Hz to 5 MHz. The surface of the sample was electroded on both opposite faces with high-grade silver paste to promote good electrical conduction. The dielectric constant of the crystal can be calculated using the following relation,

$$\epsilon r = Ct/A\epsilon_0 \quad (3)$$

where  $C$  is the capacitance of the crystal,  $t$  is the thickness of the crystal,  $\epsilon_0$  is the absolute permittivity of the free face ( $8.854 \times 10^{-12}$  F/m),  $A$  is the area of the crystal and  $\epsilon r$  is the dielectric constant of the crystal. Fig. 13 shows the variations of dielectric constant ( $\epsilon r$ ) with log frequency. From the graph, the value of dielectric constant decreases with the increase in frequency for all temperature and then remains constant at higher frequencies. The high value of dielectric constant of DEASI crystal at low frequencies may be attributed to the contribution of polarizations, namely, space charge, orientational, electronic and ionic polarizations and its low value at higher frequencies may be due to the loss of significance of these polarizations gradually. From the graph, the dielectric constant is seen to increase with an increase of temperature, and this ascribed to space charge polarization near the grain boundary interfaces, which depends on the purity and perfection of the crystal [26]. The very low value of dielectric constant at higher frequencies is important for the fabrication of materials towards photonic, electro-optic devices and NLO applications.

Fig. 14 shows the variation of dielectric loss of the grown crystal with frequency at different temperature. It is seen from the figure the dielectric loss values are found to be high at low frequencies and further decreases with an increase in high frequencies. The behavior of low value dielectric loss with high frequency for DEASI crystals suggests that the crystal possesses enhanced optical quality with lesser defects, which is the desirable property for the fabrication of nonlinear optical materials in their field of applications [27]. Thus, the results suggest that the dielectric constant and loss strongly depend on the frequency and the temperature of the crystal.

#### Etching studies

The chemical etching studies were carried out to analyse crystal growth mechanism and crystal defects. The (010) faces of DEASI have been completely dipped at room temperature in the mixed etchant of methanol and acetonitrile for a period of 5, 10 and 15 s, and then surface etchant was removed gently using tissue paper. Afterwards, the feature of the crystal surface was examined under an optical microscope reflection mode which is shown in the Fig. 15a–d. Fig. 15(a) shows the surface features of the DEASI as grown single crystal before etching. From the Fig. 15b–d, it is seen that the number of low angle grain boundaries and etch pits

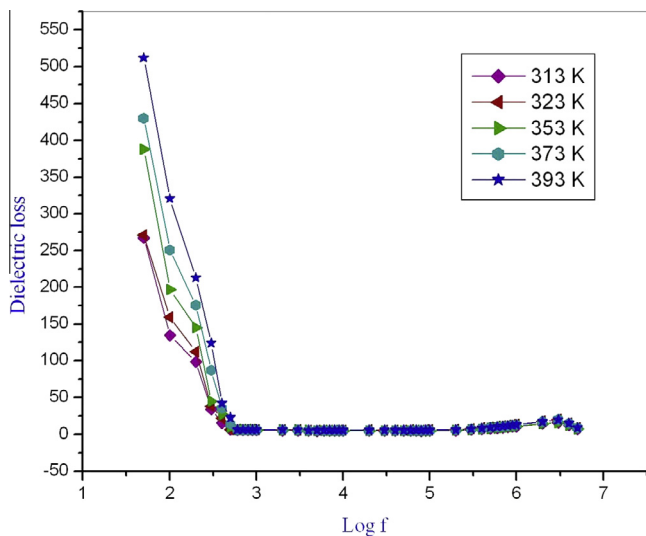


**Fig. 14.** Variation of dielectric loss with log frequency at different temperatures for DEASI single crystal.

have been identified which are clearly visible. The low angle grain boundaries occurred may be due to segregation of impurities on the surface of the grown crystal [28]. Thus, the observed etch pits suggest that DEASI crystal is in a layer growth, confirm the two dimensional (2D) growth mechanisms with increasing size of the pattern with increasing the etching time, and fewer dislocations [29].

### SHG measurement

#### Kurtz and Perry technique

The second harmonic generation test of DEASI crystals was examined by Kurtz and Perry powder method [30]. A high density Q-switched Nd: YAG laser emitting radiation of wavelength 1064 nm with pulse width an input repetition rate of 10 Hz and energy 4.6 mJ/pulse was allowed to fall onto the powdered sample in a Capillary tube using visible blocking filter. This experiment shows the lack of greenish emission of radiation for DEASI (zero second order NLO response). So, this test reveals that the centrosymmetry nature of the crystal, but no symmetry restrictions are there for to fulfill the third order NLO applications [31].

### Conclusion

Bulk crystals of a stilbazolium derivative 2-(4-Diethylamino-phenyl)-vinyl]-1-methyl-pyridinium iodide were synthesized, and the crystals were grown by slow evaporation technique at 35 °C. Single crystal X-ray diffraction study has been performed to determine the lattice parameter and the crystal system. The grown crystal belongs to the monoclinic crystal system with centrosymmetric space group P2(1)/c. The functional groups and formation of the electronic structure were confirmed from FT-IR,  $^1\text{H}$  NMR and  $^{13}\text{C}$  NMR analysis. The UV–Vis NIR spectrum shows, its absorption takes place in UV region and transmittance nature in the Vis–NIR region. The refractive index ( $n$ ) value was found at 1.647. Thermal behavior of DEASI was studied by TGA/DSC analysis and its reveals that the material is decomposes at 276.6 °C. Mechanical properties of the grown crystal were studied by using

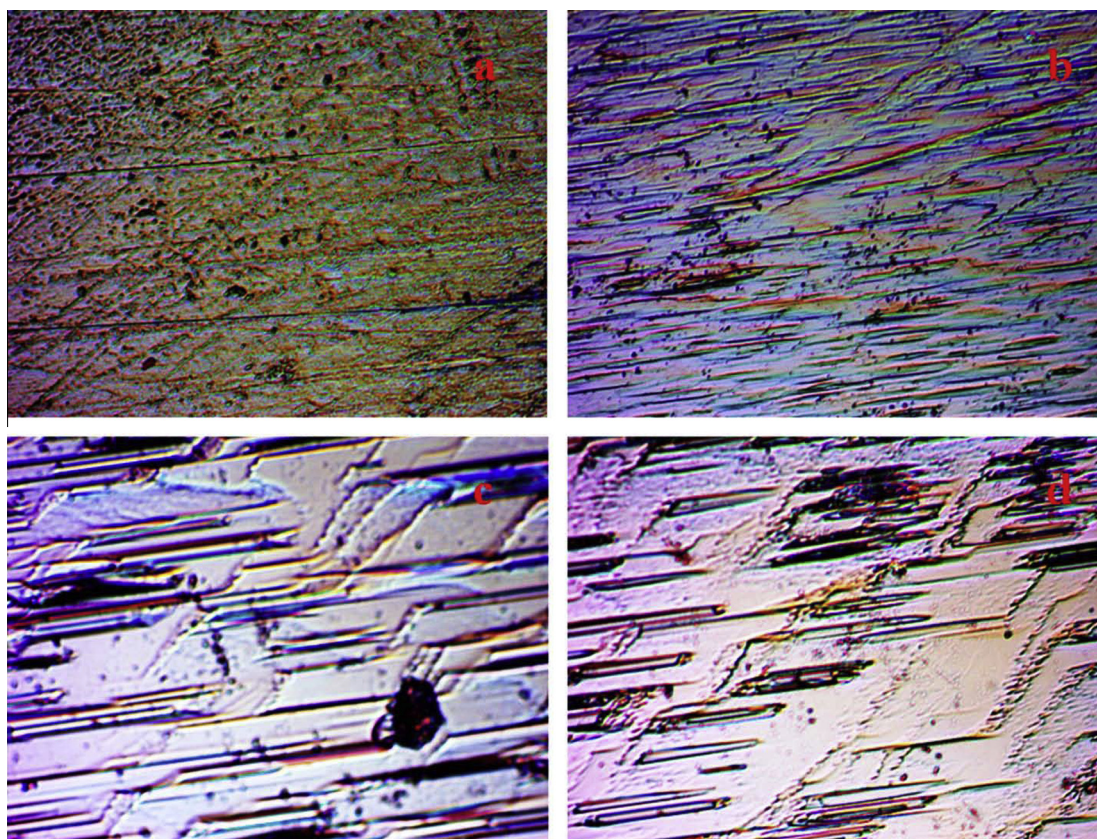


**Fig. 15.** Chemical etching time of DEASI single crystal on (010) face with methanil and acetonitrile mixed solvent as an etchant (a) as grown surface, (b) 5 s, (c) 10 s and (d) 15 s.

Vicker's micro hardness technique, and DEASI crystal falls in a soft material category. Dielectric studies revealed that dielectric constant and dielectric loss of the grown crystal decrease with increase of frequencies. The chemical etching studies shows that the perfection and quality of grown crystal is good. All these properties show that this compound may be a promising material for applications in nonlinear optical area.

### Acknowledgements

The authors wish to thank to SAIF IIT madras for providing a single crystal XRD analysis. The authors also would like to thank to Defence Research and Development Organization (DRDO), Government of India for financial support and VIT University management, Vellore for their constant support and encouragements.

### References

- [1] A.M. Petrosyan, R.P. Sukiyasan, H.A. Karpetyan, S.S. Tenzya, R.S. Feigelson, *J. Cryst. Growth* 213 (2000) 103.
- [2] S.B. Monaco, L.E. Davis, S.P. Velsko, F.T. Wong, D. Eimerl, *J. Cryst. Growth* 85 (1987) 252.
- [3] B.B. Bozena, A.V. Bree, B.O. Patrick, J.R. Scheffer, J. Trotter, *Can. J. Chem.* 76 (1998) 1616.
- [4] J.E. Reeve, H.L. Anderson, K. Clays, *Phys. Chem. Chem. Phys.* 12 (2010) 13484–13498.
- [5] C.C. Frazier, M.P. Cockerham, E.A. Chauchard, C.H. Lee, *J. Opt. Soc. Am. B* 4 (1987) 1899.
- [6] P.N. Prasad, D.J. Williams, *Introduction to Nonlinear Optical Effects in Molecules and Polymers*, Wiley Interscience, New York, 1991.
- [7] S.R. Marder, *Chem. Commun.* 2 (2006) 131–134.
- [8] J. Zyss, J.F. Nicoud, M. Coquillay, *J. Chem. Phys.* 81 (1984) 4160.
- [9] I. Ledoux, J. Badan, J. Zyss, A. Migus, D. Hulin, J. Etchepare, G. Grillon, A. Antonetti, *J. Opt. Soc. Am. B* 4 (1987) 987.
- [10] R. Gunaseelan, S. Selvakumar, P. Sagayaraj, *Scientia Acta Xaveriana* 3 (2012) 45–60.
- [11] Blanca Ruiz, J. Coe Benjamin, Reto Gianotti, Volker Gramlich, Mojca Jazbinsek, Peter Gunter, *Cryst. Eng. Commun.* 9 (2007) 772–776.
- [12] B.J. Coe, J.A. Harris, A.K. Clays, G. Olbrechts, A. Persoons, J.T. Hupp, R.C. Johnson, S.J. Coles, M.B. Hursthouse, K. Nakatani, *Adv. Funct. Mater.* 12 (2002) 110.
- [13] B. Ruiz, Z. Yang, V. Gramlich, M. Jazbinsek, P. Gunter, *J. Mater. Chem.* 16 (2006) 2839.
- [14] K. Nagaoka, H. Adachi, S. Brahadesewaran, T. Higo, M. Takagi, M. Yoshimura, Y. Mori, T. Sasaki, *Jpn. J. Appl. Phys.* 43 (2004) L261.
- [15] Narissara Kaewmanee, Kullapa Chanawanno, Suchad Chantraprommaa, Hoong-Kun Fun, *Acta Cryst. E* 66 (2010) o2639–o2640.
- [16] W. Kaminsky, *J. Appl. Cryst.* 38 (2005) 566.
- [17] W. Kaminsky, *J. Appl. Cryst.* 40 (2007) 382.
- [18] George Socrates, *Infrared and Raman Characteristic Group Frequencies – Tables and Charts*, third ed., John Wiley and Sons Ltd., England, 2001. 5.
- [19] R. Jerald Vijay, N. Melikechi, Tina Thomas, R. Gunaseelan, M. Antony Arockiaraj, P. sagayaraj, *Mater. Chem. Phys.* 132 (2012) 610–617.
- [20] K. Kumar, R. Rai, S.B. Rai, *Appl. Phys. B Lasers Opt.* 96 (2009) 85–94.
- [21] K. Jagannathan, S. Kalainathan, *J. Cryst. Growth* 310 (2008) 2043–2049.
- [22] T. Uma devi, N. Lawrence, R. Ramesh babu, K. Ramamurthi, *J. Cryst. Growth* 310 (2008) 116–123.
- [23] E.M. Onitsch, *Mikroskopie* 95 (1998) 12.
- [24] S. Karan, S.P.S. Gupta, *Mater. Sci. Eng. A* 398 (2005) 198–203.
- [25] S. Boomadevi, H.P. Mittal, R. Dhanasekaran, *J. Cryst. Growth* 261 (2004) 55.
- [26] C.P. Smyth, *Dielectric Behavior and Structure*, McGraw-Hill, New York, 1965. 132.
- [27] C. Balarew, R. Duhlev, *J. Solid State Chem.* 55 (1984) 1.
- [28] M. SenthilPandian, P. Ramasamy, *J. Cryst. Growth* 312 (2010) 413–419.
- [29] T. Mukerji, J. Kar, *J. Cryst. Growth* 204 (1999) 341.
- [30] S.K. Kurtz, T.T. Perry, *J. Appl. Phys.* 39 (1968) 3798–3813.
- [31] K. Vanchinathan, G. Bhagavannarayana, K. Muthu, S.P. Meenakshisundaram, *Physica B* 406 (2011) 4195–4199.